Electronic Supplementary Information

Carboxamide functionality grafted entangled Co(II) framework as a unique hydrogen-bond-donor catalyst in solvent-free tandem deacetalization-Knoevenagel condensation with pore-fitting-mediated size-selectivity

Partha Pratim Mondal[a], Nilanjan Seal[a,b], Manpreet Singh[a,b], Subhadip Neogi[a,b,*]

[a]Inorganic Materials & Catalysis Division, CSIR-Central Salt & Marine Chemicals Research Institute, Bhavnagar, Gujarat 364002, India
[b]Academy of Scientific and Innovative Research (AcSIR), Ghaziabad- 201002, India
**E-mail address*: sneogi@csmcri.res.in, subhadip79@gmail.com

Table of contents

Materials and Physical measurements

All the solvents and reagents were purchased from commercial sources (except H_3TCA) and used without further purification. Powder X-ray diffraction (PXRD) data were collected using a PANalytical Empyrean (PIXcel 3D detector) system equipped with Cu Kα (λ=1.54 Å) radiation. The Fourier Transform Infrared-spectra (IR) of the samples were recorded using the KBr pellet method on a Perkin–Elmer GX FTIR spectrometer in the region of 4000−400 cm^{-1}. Thermogravimetric analyses (TGA) (heating rate of 5 °C/min under N_2 atmosphere) were performed with a Mettler Toledo Star SW 8.10 system. Surface area measurement was carried out using Quantachrome Autosorb IQ instrument. ^1H and ^{13}C NMR spectra were recorded on a Bruker Avance-II 500 MHz NMR spectrometer. Scanning Electron Microscopic (SEM) and Transmission Electron Microscopic (TEM) images were obtained with a JEOL JSM 7100F and JEOL, JEM 2100 instrument, respectively. XPS analysis was carried out using a Thermo Scientific ESCALAB 250 Xi photoelectron spectrometer (XPS) using a monochromatic Al Kα X-ray as an excitation source. Inductively coupled plasma-mass spectrometry (ICP-MS) analysis was measured by Perkin Elmer, Optima 2000.

Single Crystal X-ray Crystallography

Single crystals with suitable dimensions were chosen under an optical microscope and mounted on a glass fibre for data collection. The crystal data for **CSMCRI-MOF-25** were collected on a Bruker D8 Quest diffractometer, with CMOS detector in shutter less mode. The crystals were cooled to low temperature using an Oxford Cryostream liquid nitrogen cryostat. The instrument was equipped with a graphite monochromatized MoKα X-ray source (λ = 0.71073 Å), with Triumph™ X-ray source optics. Data collection and initial indexing and cell refinement were handled using APEX II software.[1] Frame integration, including Lorentz-polarization corrections, and final cell parameter calculations were carried out using SAINT+ software.[2] The data were corrected for absorption using the SADABS program.[3] Decay of reflection intensity was monitored by analysis of redundant frames. The structure was solved using Direct methods and difference Fourier techniques. All non-hydrogen atoms were refined anisotropically. All H atoms were placed in calculated positions using idealized geometries (riding model) and assigned fixed isotropic displacement parameters. The SHELXL-2014 package within the OLEX2 crystallographic software[4] was applied for structure refinement with several full-matrix least-squares/difference Fourier cycles.[5] The disordered guest solvent molecules in the crystal lattice were treated with solvent mask option in OLEX2 software.[4] The potential solvent accessible void space was calculated using the PLATON[6] software. The crystal and refinement data for **CSMCRI-MOF-25** is listed in Table S1. Topological analysis

was performed by using ToposPro software.[7] Structures of reactant molecules were drawn and optimized using Avogadro software.[8]

Synthesis of the ligand. The ligand was prepared and characterized according to literature reported method.[9]

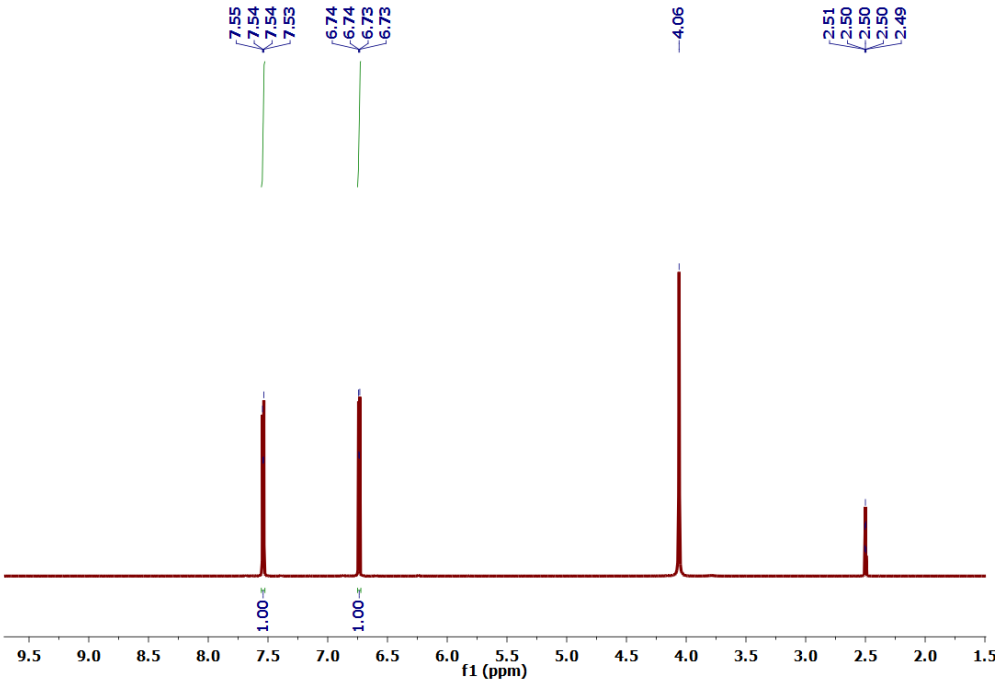

Fig. S1 ^{1}H NMR spectrum of 1,3-di(pyridin-4-yl)urea in DMSO-d_6.

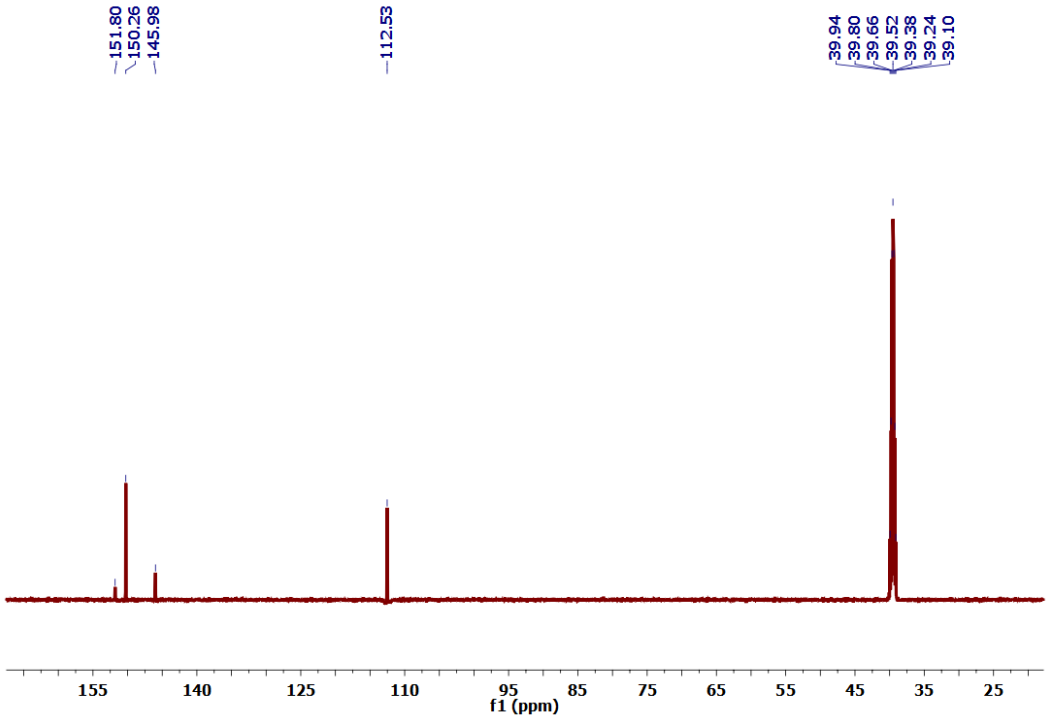

Fig. S2 ^{13}C NMR spectrum of 1,3-di(pyridin-4-yl)urea in DMSO-d_6.

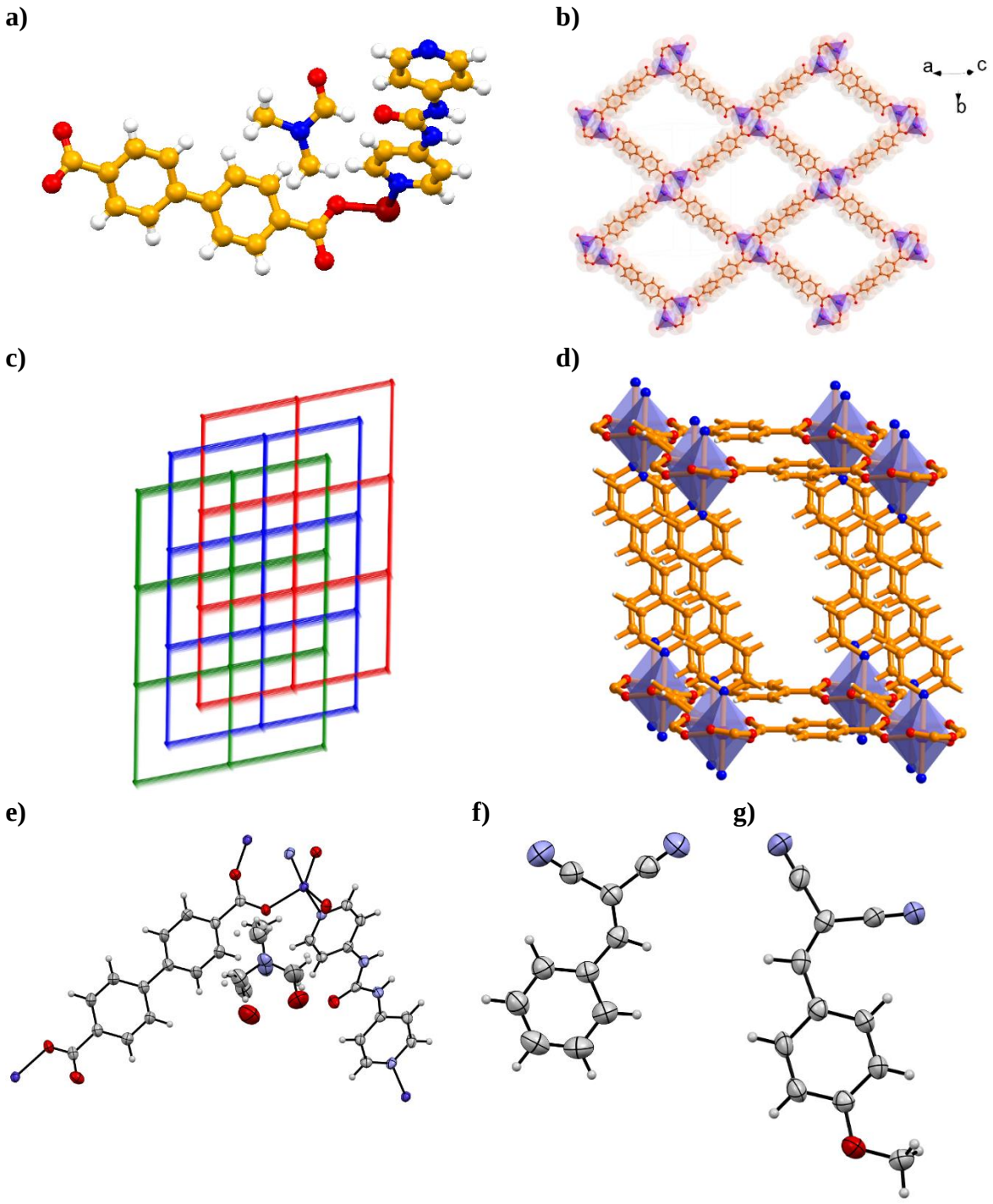

Fig. S3 (a) Asymmetric unit of **CSMCRI-MOF-25**. (b) Two-dimensional (2D) layer of the MOF. (c) Topological representation of **CSMCRI-MOF-25**. (d) Structure of the un-functionalized MOF (**UN-MOF**). ORTEP diagram of (e) **CSMCRI-MOF-25**, (f) **1C** and (g) **3C**.

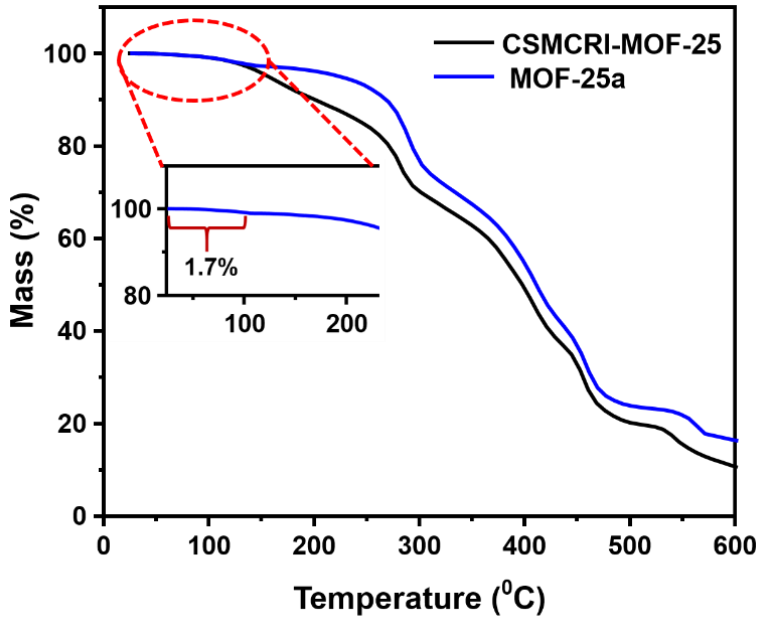

Fig. S4 Thermogravimetric analysis (TGA) of as-synthesized and activated **CSMCRI-MOF-25** (inset shows the trapped water).

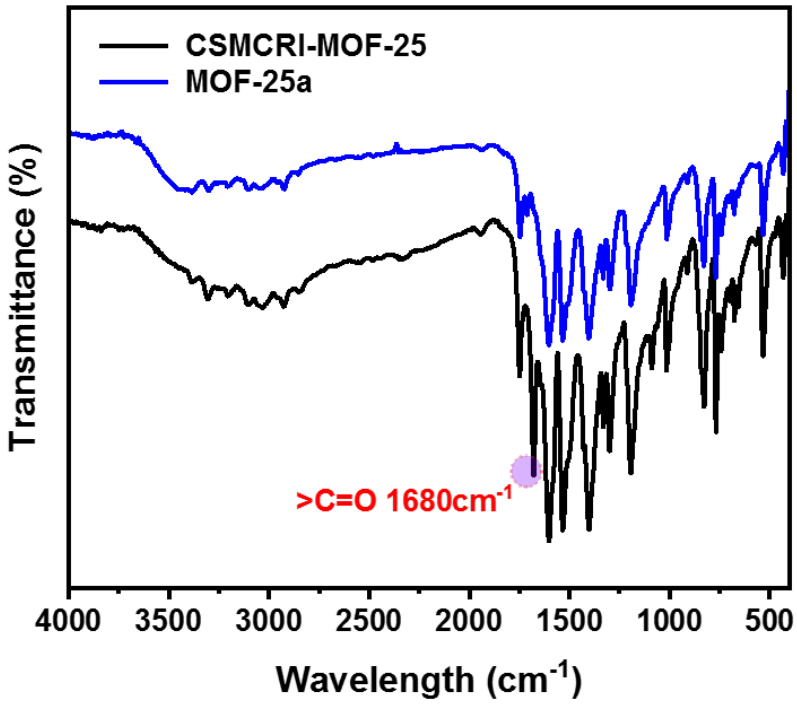

Fig. S5 FT-IR profile of as-synthesized and activated **CSMCRI-MOF-25**.

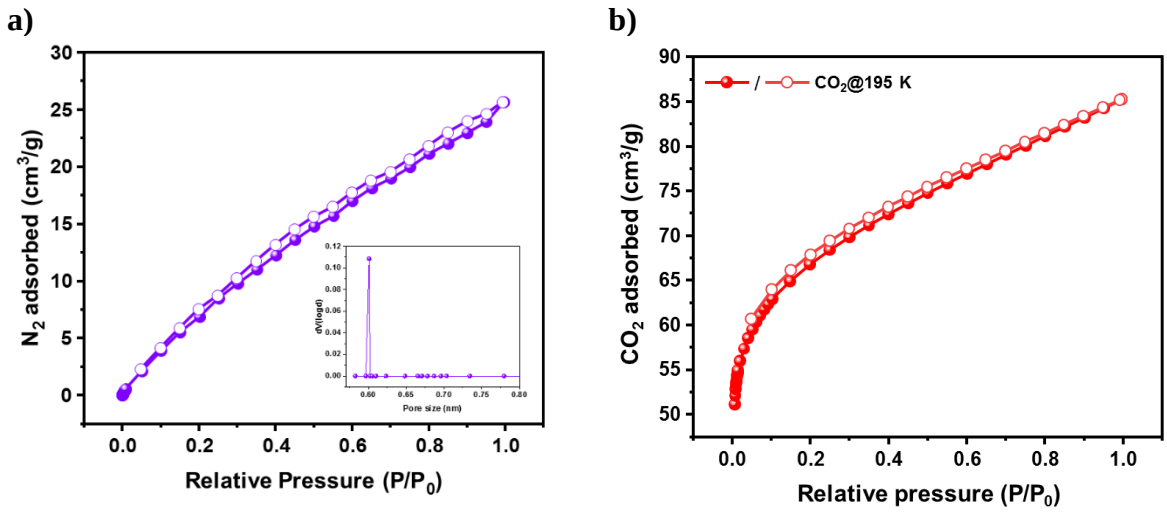

Fig. S6 Adsorption isotherm of activated **CSMCRI-MOF-25** for (a) N_2 at 77 K (inset shows pore-size distribution) and (b) CO_2 at 195 K.

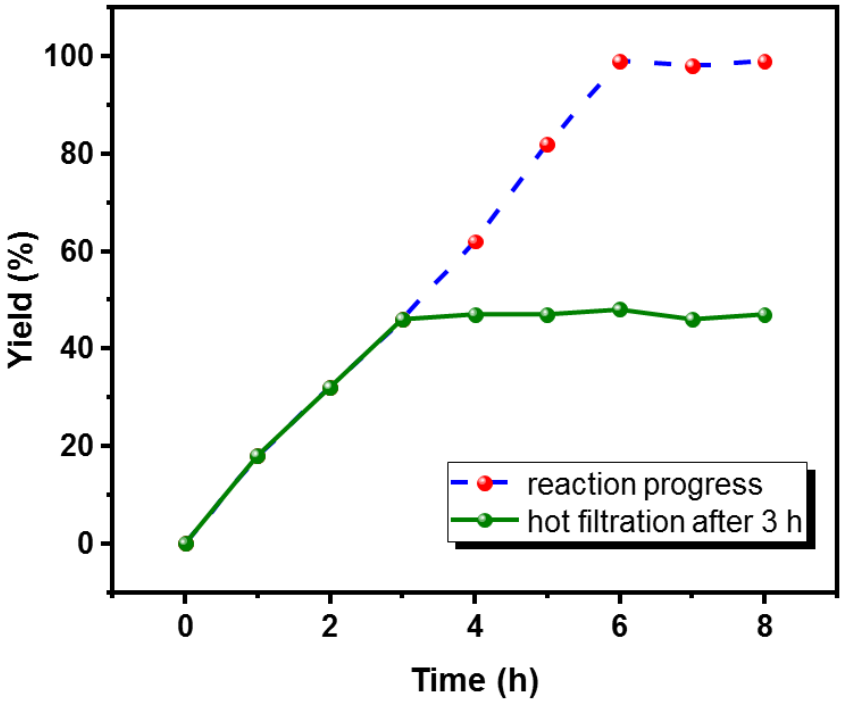

Fig. S7 Hot-filtration test for tandem deacetalization-Knoevenagel condensation reaction.

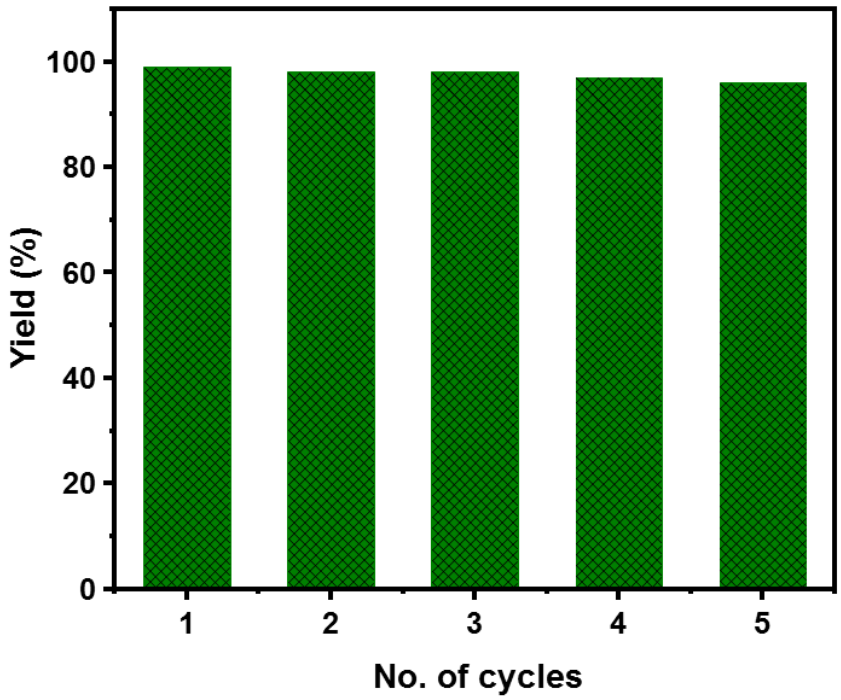

Fig. S8 Recyclability test of the catalyst up to five cycles in tandem deacetalization-Knoevenagel reaction, showing negligible loss in catalytic activity.

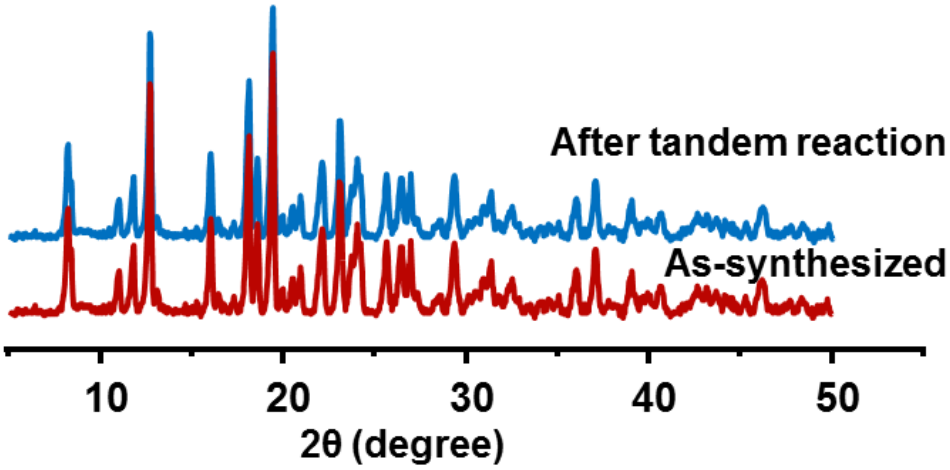

Fig. S9 PXRD pattern of the MOF, obtained after tandem deacetalization-Knoevenagel reaction.

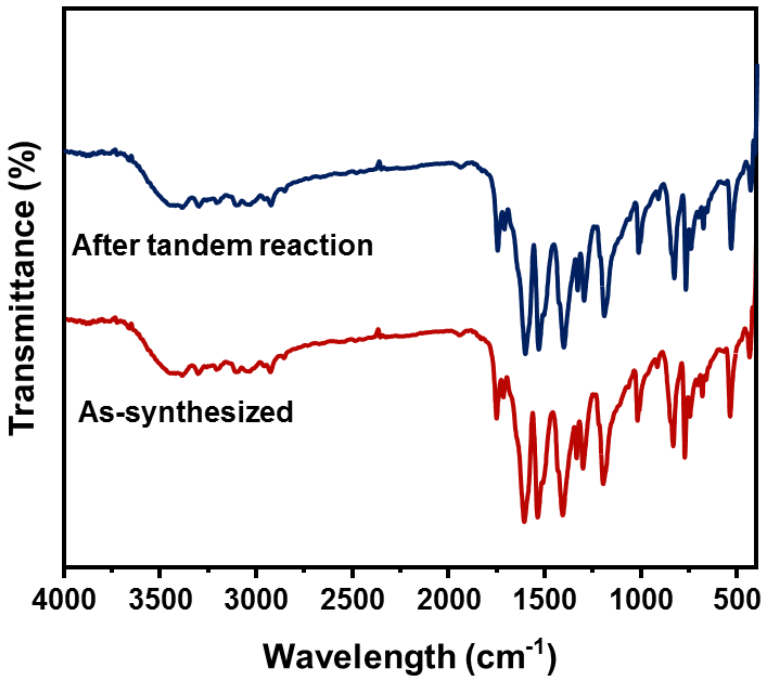

Fig. S10 FT-IR profile of the MOF, obtained after tandem deacetalization-Knoevenagel reaction.

a) **b)**

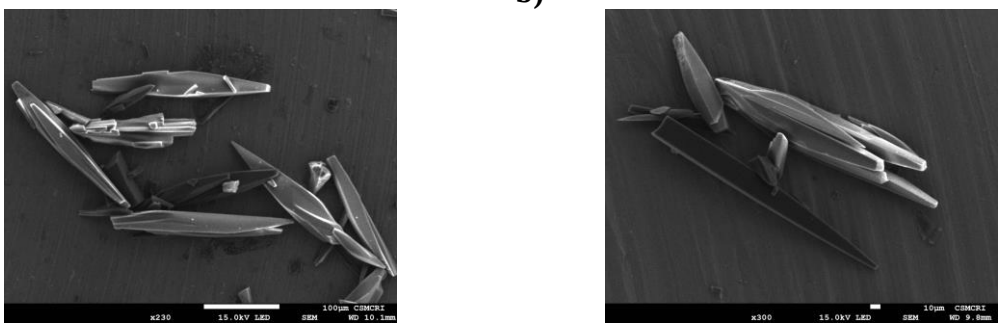

Fig. S11 FE-SEM image of the MOF (a) before and (b) after tandem deacetalization-Knoevenagel reaction.

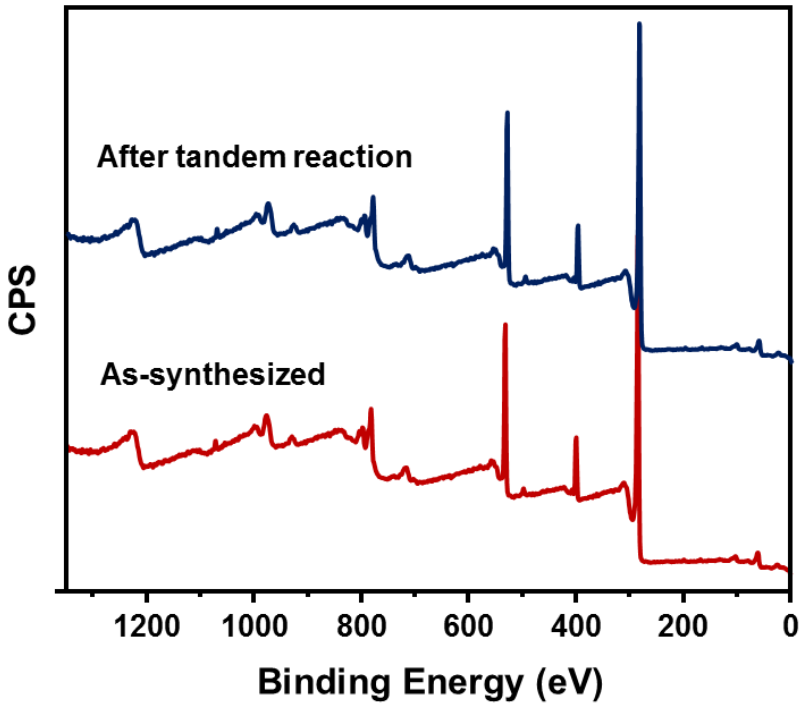

Fig. S12 XPS survey spectra of the MOF before and after tandem deacetalization-Knoevenagel reaction.

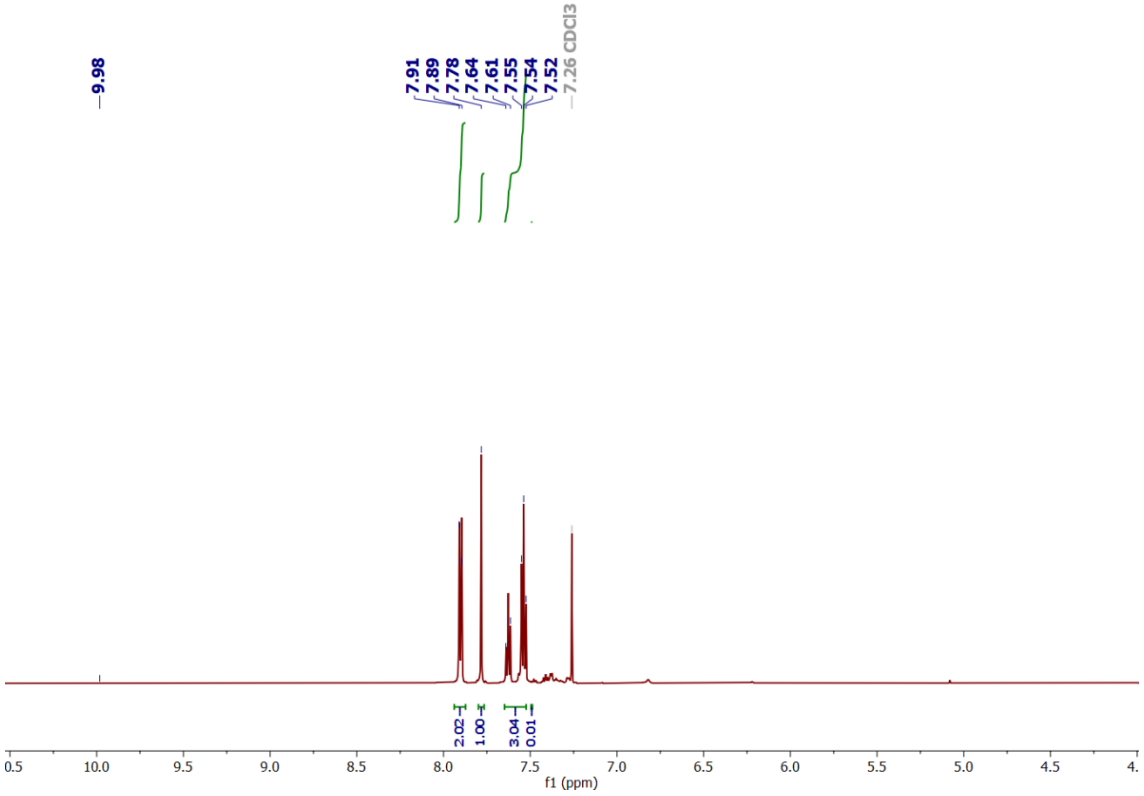

Fig. S13 ^{1}H NMR of the model product (**1C**) of tandem deacetalization-Knoevenagel condensation.

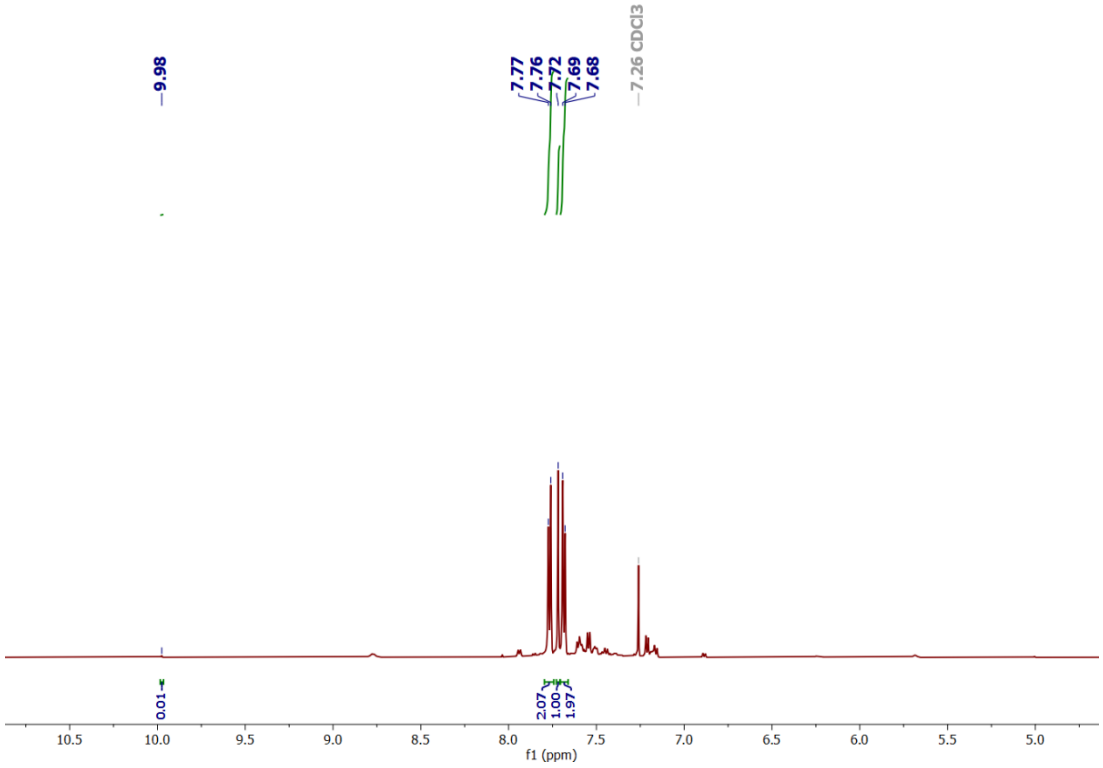

Fig. S14 ^{1}H NMR of *p*-bromobenzyledine malononitrile (**2C**).

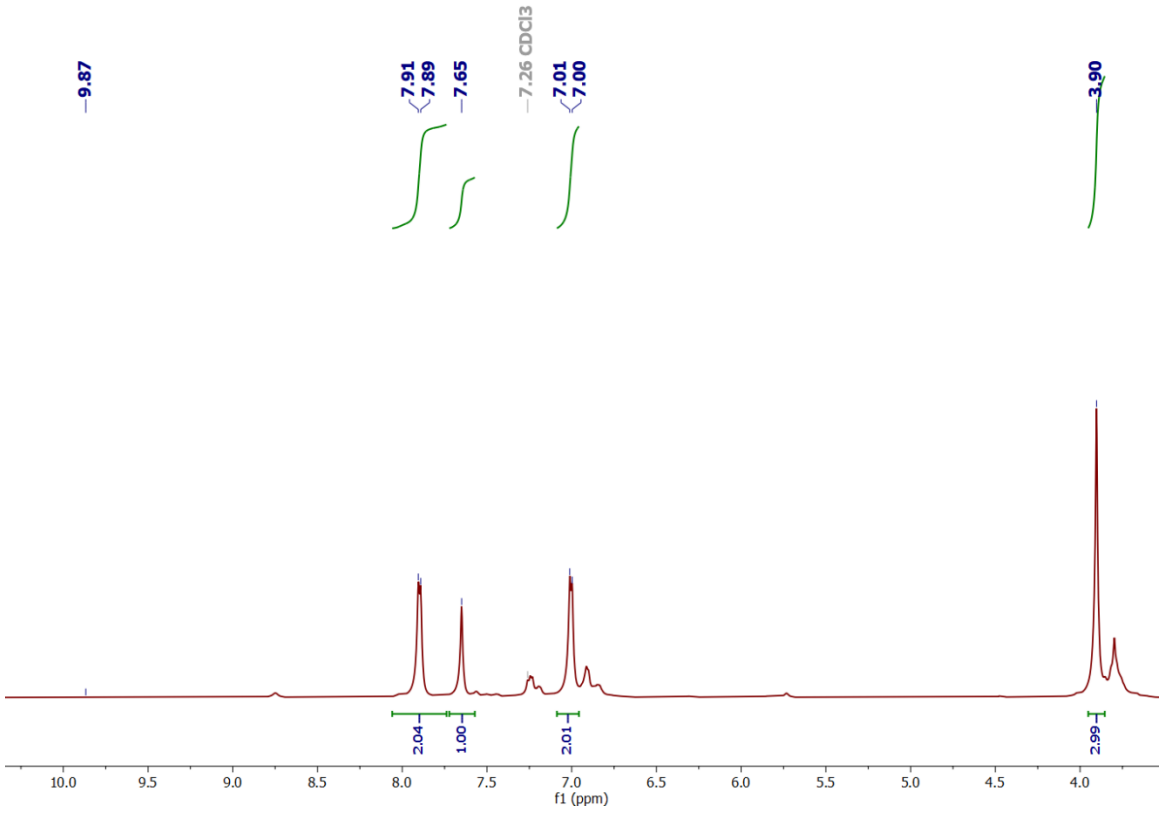

Fig. S15 ^{1}H NMR of *p*-methoxybenzyledine malononitrile (**3C**).

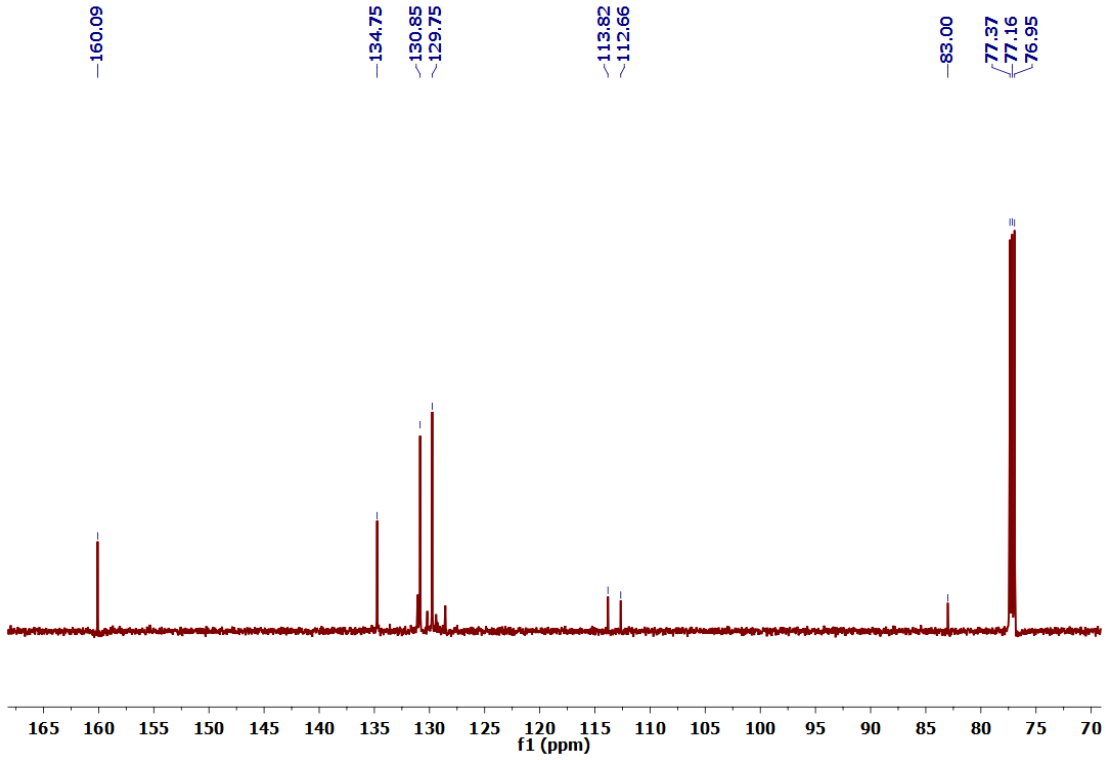

Fig. S16 ^{13}C NMR of the model product (**1C**) of tandem deacetalization-Knoevenagel condensation.

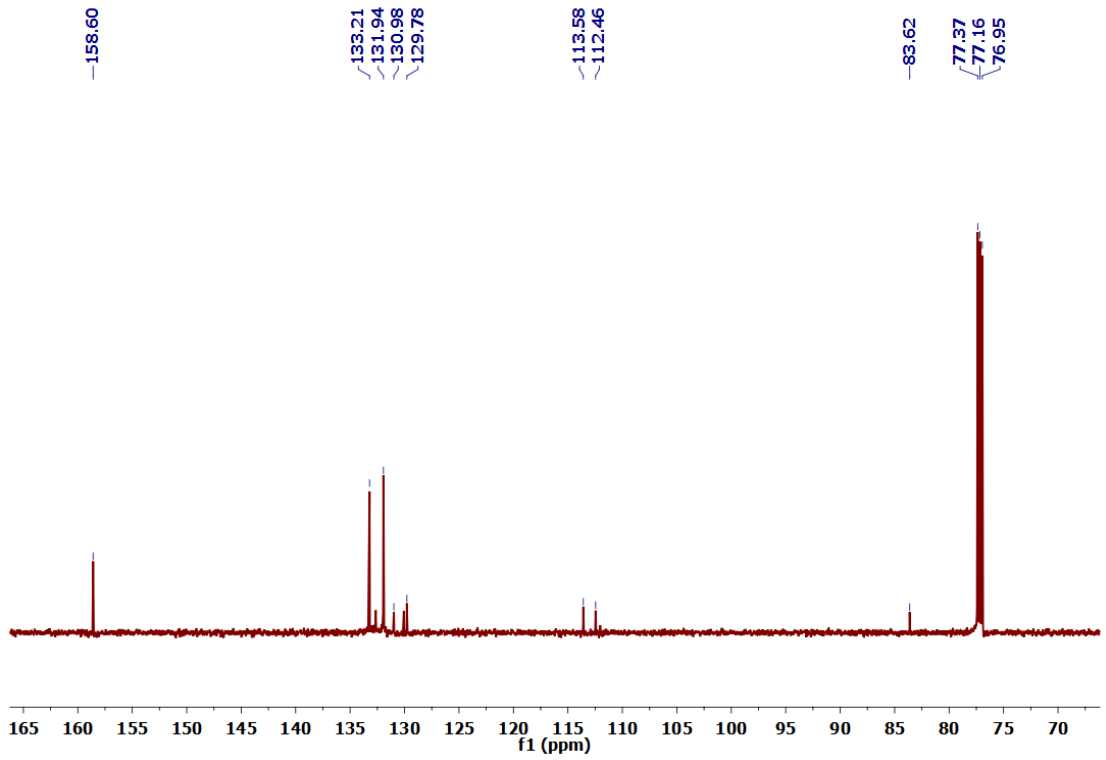

Fig. S17 ^{13}C NMR of *p*-bromobenzyledine malononitrile (**2C**).

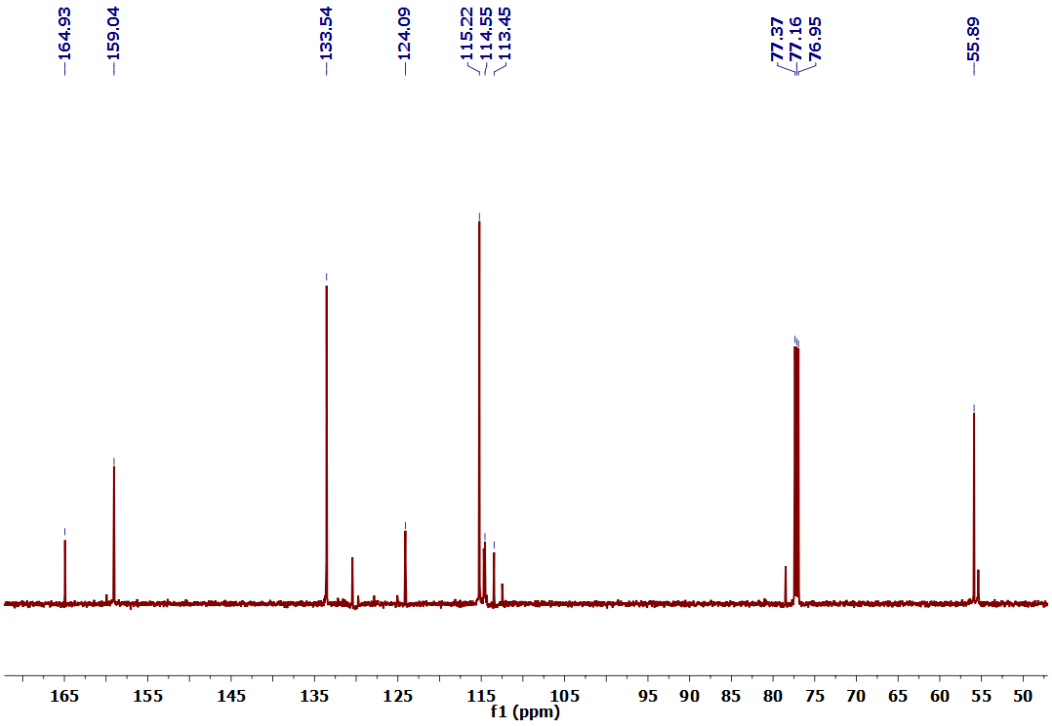

Fig. S18 ^{13}C NMR of *p*-methoxybenzyledine malononitrile (**3C**).

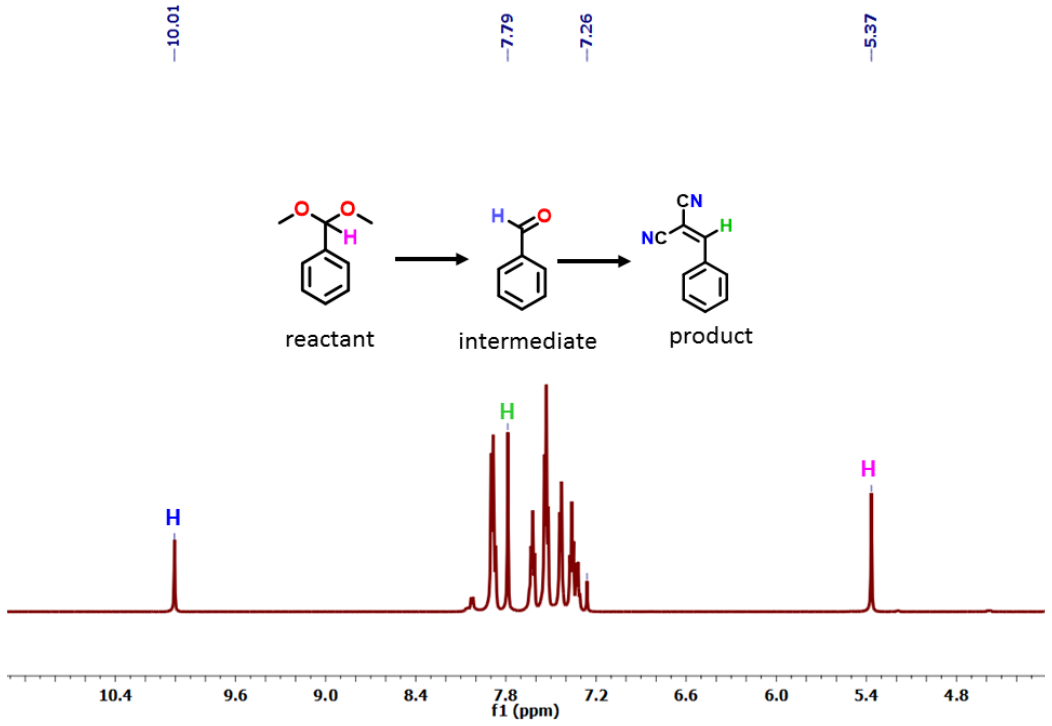

Fig. S19 ^{1}H NMR spectrum of the aliquot, withdrawn after 3 h of reaction, showing the formation of intermediate benzaldehyde.

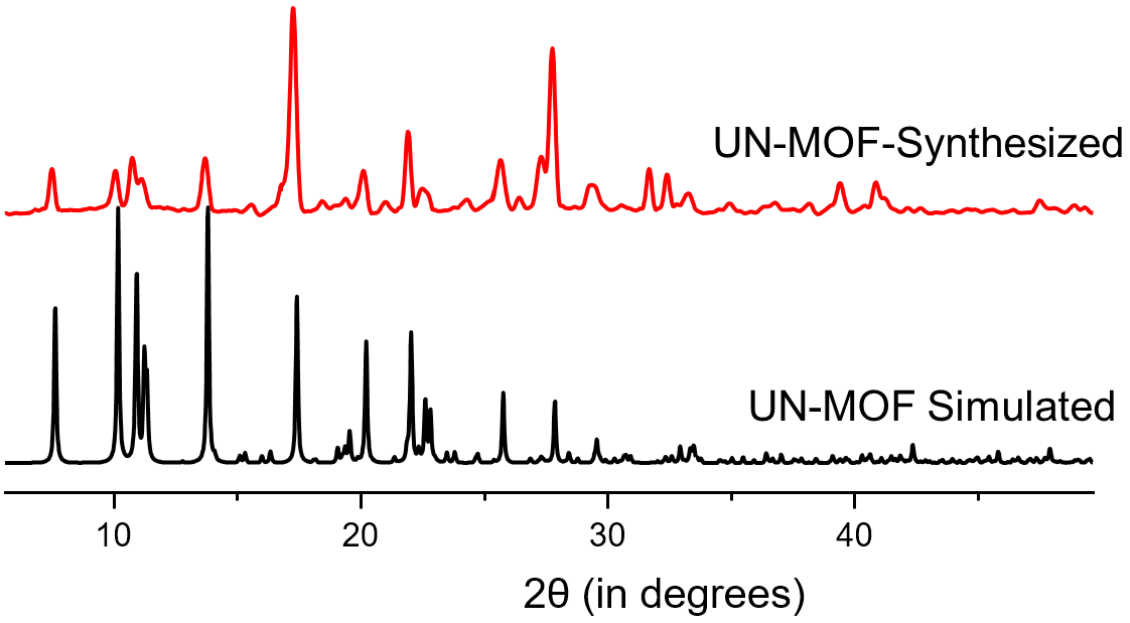

Fig. S20 Comparison of PXRD patterns of **UN-MOF** (simulated and as-synthesized).

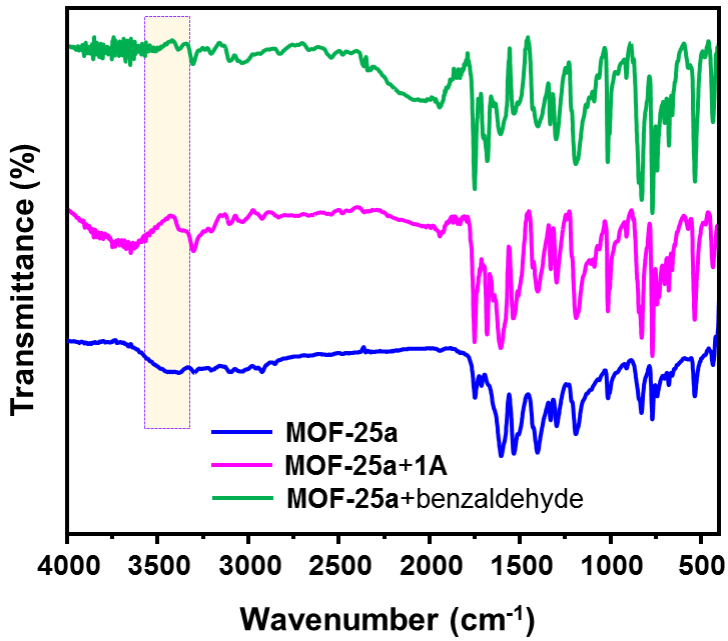

Fig. S21 FT-IR profile of (**MOF-25a**+**1A**) and (**MOF-25a**+benzaldehyde), showing decrease in N-H band intensity along with its and shifts towards lower wavenumber, corroborating H-bonding interaction between N-H groups of **MOF-25a** and **1A** and/or benzaldehyde.

Table S1. Crystal data and refinement parameters for **CSMCRI-MOF-25**, **1C** and **3C**

Identification code	**CSMCRI-MOF-25**	**1C**	**3C**
Empirical formula	$C_{28}H_{25}CoN_5O_6$	$C_{10}H_6N_2O$	$C_{11}H_8N_2O$
Formula weight	586.47	154.17	184.20
Temperature/K	293(2)	301.15	298.0
Crystal system	monoclinic	monoclinic	monoclinic
Space group	$P2_1/c$	$P2_1/c$	$P2_1/c$
a/Å	10.7124(4)	9.3728(14)	3.9384(12)
b/Å	21.0705(9)	3.9812(7)	24.989(7)
c/Å	12.0672(4)	22.161(4)	9.674(3)
α/°	90	90	90
β/°	99.579(4)	93.573(5)	90.874(12)
γ/°	90	90	90
Volume/$Å^3$	2685.78(17)	825.3(2)	952.0(5)
Z	4	4	4
$\rho_{calc}g/cm^3$	1.4503	1.2407	1.2850
μ/mm^{-1}	0.691	0.077	0.085
F(000)	1214.3	320.1	384.2
Crystal size/mm^3	0.14 × 0.09 × 0.02	0.78 × 0.203 × 0.06	0.9 × 0.5 × 0.06
Radiation	Mo Kα (λ = 0.71073)	Mo Kα (λ = 0.71073)	Mo Kα (λ = 0.71073)
2Θ range for data collection/°	5.1 to 50	4.36 to 60.94	4.52 to 49.98
Index ranges	$-16 \le h \le 13$, $-25 \le k \le 31$, $-17 \le l \le 18$	$-13 \le h \le 13$, $-5 \le k \le 5$, $-31 \le l \le 31$	$-5 \le h \le 5$, $-34 \le k \le 34$, $-13 \le l \le 13$
Reflections collected	20283	11923	55753
Independent reflections	4720 [R_{int} = 0.0346, R_{sigma} = 0.0507]	2513 [R_{int} = 0.0772, R_{sigma} = 0.0670]	1677 [R_{int} = 0.1089, R_{sigma} = 0.0428]
Data/restraints/parameters	4720/82/410	2513/0/134	1677/0/128
Goodness-of-fit on F^2	1.053	1.062	2.157
Final R indexes [I>=2σ (I)]	R_1 = 0.0497, wR_2 = 0.1290	R_1 = 0.0610, wR_2 = 0.1511	R_1 = 0.1348, wR_2 = 0.4278
Final R indexes [all data]	R_1 = 0.0566, wR_2 = 0.1382	R_1 = 0.1354, wR_2 = 0.2069	R_1 = 0.1367, wR_2 = 0.4305
Largest diff. peak/hole / e $Å^{-3}$	1.20/-0.58	0.29/-0.27	0.54/-0.70

Determination of formula & solvent composition of CSMCRI-MOF-25 from PLATON Squeeze and Thermogravimetric analysis data

From the TGA plot of as-synthesized **CSMCRI-MOF-25**, the observed mass loss is 10.4 %

From PLATON Squeeze program void electron count / unit cell comes out to be 0

As DMF, and Methanol were used as solvents during the synthesis of the MOF, so the void space should be occupied by these lattice solvent molecules.

Now, formula of the asymmetric unit excluding guest solvents is [Co(*BPDC*)(***L***)] and mass of this asymmetric unit is 513.37.

Considering the above mentioned number of electrons, the best possible combination of solvent molecules for **CSMCRI-MOF-25** could be [Co(*BPDC*)(***L***)]·DMF

The aforementioned combination was further cross-checked from TGA analysis.

Mass loss due to lattice solvents is [(73×1)] = 73

Therefore, total mass of **CSMCRI-MOF-25** including lattice solvents is = 586.37

Mass loss due to lattice DMF molecules thereafter is [(73×1)/586.37] ×100 % = 12.45 % which is in good agreement with that of the experimental TGA results.

Table S2. A comparison of catalytic activity of **CSMCRI-MOF-25** with various other systems in tandem deacetalization-Knoevenagel condensation reaction

Entry	Catalyst	Solvent/temperature/time/ catalyst amount	Yield (%)	References
1.	$[Cd_3(\boldsymbol{L})_2(dpa)(DMA)(H_2O)]$	Solvent-free/ 60 °C / 4 h/ 1.18 mol%	>99	*Mater. Today Chem.* **2022**, *26*, 101064
2.	$(CH_3)_2NH_2{\cdot}[Co_3(TCA)_2(\mu_2\text{-}OH)(bpy)1.5(H_2O)_3]$	DMSO-d_6/60 °C/ 6 h/ 1.26 mol %	97.08	*ACS Appl. Mater. Interfaces* **2021**, *13*, 28378-28389
3.	MIL-101(Cr)@CS in situ growth method [MIL-101(Cr)/CS = 2.86]	Acetonitrile/ 80 °C/ 12 h/ 50 mg	99	*ACS Appl. Nano Mater.* **2020**, *3*, 6316−6320
4.	MIL-101(Al/Fe)-NH_2(20:1)	Toluene/ 90 °C/ 1.5 h/ 20 mg	99.8	*Catal. Sci. Technol.* **2020**, *10*, 315–322
5.	(PCN-222-Co@TpPa-1)	DMSO-d_6/50 °C/ 10 h/ 5 mg	99.3	*Chem. Commun.* **2019**, *55*, 6377--6380
6.	$[Cd_3(C_8H_3SO_7)_2\text{-}(C_{10}H_8N_4)_3(C_3H_7NO)_2](C_3H_7NO)_2{\cdot}(CH_3OH)_4$	DMF/ 90 °C/ 5 h/ 0.56 mol%	84	*Cryst. Growth Des.* **2019**, *19*, 747−755
7.	UiO-66@SNW-1	DMSO-d_6/80 °C/ 12 h/ 50 mg	99.6	*Inorg. Chem.* **2018**, *57*, 14467−14470

8.	Cu-HNUST-8	DMSO/50 °C/48 h/0.5 mol%	99	*Inorg. Chem. Front*. **2018**, *5*, 2355−2363
9.	Sm-BDC-NH_2	DMSO/ 50 °C/ 24 h/ 2 mol%	76	*Inorg. Chem*. **2018**, *57*, 2193–2198
10.	PBSA/Cr-MIL-101 + PMAP/Cr-MIL-101	DMSO+water/ 70 °C/ 12 h/ 5 mol%	89	*Chem. - Eur. J*. **2018**, *24*, 9903−9909
11.	JUC-199	1,4-Dioxane/90 °C/ 4 h/ 100 mg	≥99.9	*J. Mater. Chem. A* **2016**, *4*, 15240–15246
12.	Cr-MIL-101-AB-x	DMF/ 90 °C/ 2 h/ 4 mol%	>91	*Inorg. Chem*. **2016**, *55*, 5753−5755
13.	PCN-124	DMSO-d_6/50 °C/ 12 h/ 0.5 mol %	~100	*Chem Comm*. **2012**, *48*, 9995
14.	**CSMCRI-MOF-25**	Solvent-free/ 60 °C / 6 h/ 10 mol%	>99	**This work**

References

1 *APEX2*, v. 2014.7-1; Bruker AXS: Madison, WI, 2014.

2 *SAINT*, v. 8.34A; Bruker AXS: Madison, WI, 2013.

3 *SADABS*, v. 2014/3; Bruker AXS: Madison, WI, 2013.

4 O. V. Dolomanov, L. J. Bourhis, R. J. Gildea, J. A. K. Howard and H. Puschmann, *J. Appl. Crystallogr.*, 2009, **42**, 339−341.

5 G. M. Sheldrick, *SHELXTL* Version 2014/7. *https://shelx.uniac.gwdg.de/SHELX/index.php.*

6 A. L. Spek, *PLATON*; The University of Utrecht: Utrecht, The Netherlands, 1999.

7 http://www.topos.ssu.samara.ru; V. A. Blatov, IUCrCompCommNewsletter 2006, 7, 4.

8 M. D. Hanwell, D. E. Curtis, D. C. Lonie, T. Vandermeersch, E. Zurek and G. R. Hutchison, *J. Cheminform.*, 2012, **4**, 17 (DOI: 10.1186/1758-2946-4-17).

9 M. Singh and S. Neogi, *Inorg. Chem.*, 2023, **62**, 871-884.